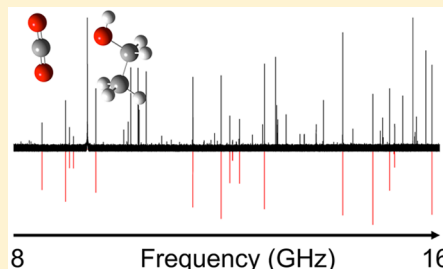


Electron Donor–Acceptor Nature of the Ethanol–CO<sub>2</sub> DimerBrett A. McGuire,<sup>\*,†,‡,§,¶</sup> Marie-Aline Martin-Drumel,<sup>‡,§</sup> and Michael C. McCarthy<sup>\*,†,‡,¶</sup><sup>†</sup>National Radio Astronomy Observatory, Charlottesville, Virginia 22903, United States<sup>‡</sup>Harvard–Smithsonian Center for Astrophysics and School of Engineering and Applied Sciences, Harvard University, Cambridge, Massachusetts 02138, United States

## S Supporting Information

**ABSTRACT:** Supercritical CO<sub>2</sub> is an appealing nontoxic, environmentally friendly solvent for the industrial extraction of many classes of compounds, from caffeine to natural product drug precursors to petrochemical impurities. Apolar in isolation, the ability of supercritical CO<sub>2</sub> to dissolve polar species has been empirically shown to be greatly enhanced by the addition of a small molar percentage of a polar cosolvent, often ethanol. Computational work predicts that the isolated ethanol–CO<sub>2</sub> complex can exist either in an electron-donor configuration or through a hydrogen-bonding one; yet, neither has been previously experimentally observed. Here, we demonstrate by rotational spectroscopy that the isolated, gas-phase ethanol–CO<sub>2</sub> dimer is an electron donor–acceptor complex.



## ■ INTRODUCTION

The ability of supercritical (sc) fluids to dissolve solid materials has been known since the late 1800s.<sup>1</sup> Nearly a century later, their use as industrial solvents is widespread, as demonstrated through their ability to extract caffeine from coffee,<sup>2</sup> nicotine from tobacco,<sup>3</sup> chemotherapeutic natural products from plants,<sup>4</sup> and petrochemical products from crude oil.<sup>5</sup> One particularly appealing industrial sc solvent is supercritical CO<sub>2</sub> (scCO<sub>2</sub>) because of its low toxicity, ease of reuse, and utility at near-ambient conditions, although its use is largely limited to apolar compounds. A common industrial practice is to add a polar solute, typically methanol (CH<sub>3</sub>OH) or ethanol (CH<sub>3</sub>CH<sub>2</sub>OH), at a low molar fraction which has been shown to substantially increase the ability of scCO<sub>2</sub> to dissolve polar solutes.<sup>6,7</sup> Despite the large enhancement in solubility and the widespread industrial exploitation of this effect, relatively little experimental effort has been dedicated to understanding the underlying chemical physics behind this phenomenon.

Experimental and theoretical studies have examined the structure and bonding patterns of methanol with CO<sub>2</sub> both in isolation (gas phase) and in solution (liquid, sc phase).<sup>8–11</sup> The gas-phase and solution systems anchor the two extremes of cluster formation: the 1:1 dimer and the ~1:25 (CH<sub>3</sub>OH/CO<sub>2</sub>) cluster in solution. In the gas phase, the CH<sub>3</sub>OH–CO<sub>2</sub> dimer has been unambiguously shown by microwave spectroscopy to be an electron donor–acceptor (EDA) complex.<sup>8</sup> The carbon atom of the CO<sub>2</sub> acts as a Lewis acid and accepts electron density from the hydroxyl oxygen on the methanol; such bonding interactions have also recently been referred to in the literature as “carbon bonds”.<sup>12</sup> When used as a liquid-phase cosolvent in scCO<sub>2</sub>, however, methanol is calculated to interact predominantly with CO<sub>2</sub> through a hydrogen-bonding configuration, with no reports of any EDA structures in simulations based on an empirical force field.<sup>9</sup> Indeed, previous

experimental and theoretical work has suggested that methanol may form homocomplex aggregates when used as a cosolvent in scCO<sub>2</sub>, with the CO<sub>2</sub> only partially contributing to these structures (see Stubbs and Siepmann,<sup>9</sup> Chatzis and Samios,<sup>10</sup> Xu et al.,<sup>11</sup> and references therein).

Similar studies have proposed that ethanol also forms self-aggregates within the scCO<sub>2</sub>,<sup>13</sup> but unlike methanol, the primary interaction with the scCO<sub>2</sub> solvent is proposed to be through EDA complexation, rather than any hydrogen bonding.<sup>14</sup> The EDA complex is calculated to dominate hydrogen-bonded configurations by a ratio of 4:1.<sup>14</sup> The isolated, gas-phase EDA ethanol–CO<sub>2</sub> dimer is calculated to be lower in energy than the hydrogen-bonded configuration by ~7.5 kJ/mol.<sup>14</sup> To our knowledge, however, no experimental observation of either configuration has been reported. Here, we describe a laboratory study of the isolated gas-phase ethanol–CO<sub>2</sub> dimer via rotational spectroscopy, work that has resulted in unambiguous identification of the EDA complex.

## ■ METHODS

A combined chirped-pulse (CP)/cavity-enhanced Fourier-transform microwave (FTMW) spectrometer instrument has been employed for this study; both have been described in detail elsewhere.<sup>15,16</sup> The cavity spectrometer<sup>16</sup> operates from 5 to 26 GHz and is aligned coaxially with propagation of the supersonic expansion; molecules are introduced to the chamber through a pinhole in one of the two cavity mirrors. The CP spectrometer,<sup>17</sup> which operates in the 8–18 GHz range, is aligned perpendicularly to the axis of the expansion. A pair of

Received: June 21, 2017

Revised: July 30, 2017

Published: July 31, 2017



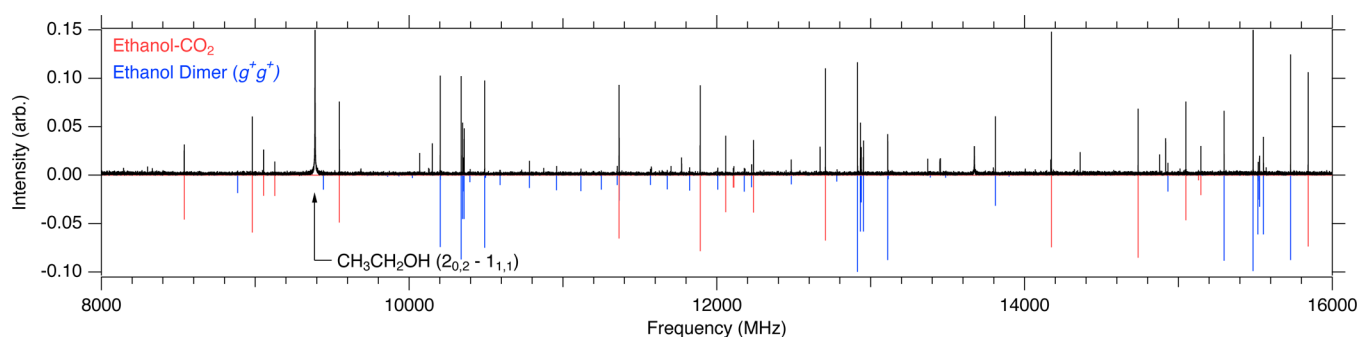


**Figure 1.** CP-FTMW spectrum of ethanol and CO<sub>2</sub> after averaging 650 000 FIDs. Instrumental artifacts have been removed. The 2<sub>0,2</sub>–1<sub>1,1</sub> transition of the ethanol monomer dominates the spectrum, and its intensity has been truncated in this plot. The g<sup>+</sup>g<sup>+</sup> conformer of the ethanol dimer is shown in blue (assignments from Loru et al.<sup>18</sup>). Transitions of the CH<sub>3</sub>CH<sub>2</sub>OH–CO<sub>2</sub> dimer assigned in this work are indicated in red. The signal-to-noise ratio for most transitions is quite high (~60).

retractable microwave absorbers is placed in front of the cavity mirror opposite the pinhole nozzle to dampen cavity resonances during CP acquisitions. The CP-FTMW spectrometer enables more than 200 000 resolution elements to be simultaneously accessed in its 10 GHz bandwidth; line centers in our spectra can be determined to an accuracy of a few 10s of kHz or better, depending on the signal-to-noise ratio. The cavity FTMW spectrometer is more than an order of magnitude more sensitive and provides frequency accuracy typically of ≤2 kHz but possesses a much narrower (~1 MHz) instantaneous bandwidth.

Gas-phase samples at a backing pressure of about 2.5 kTorr were expanded in Ar or Ne through a pulsed-nozzle supersonic expansion source, adiabatically cooling the molecules to a rotational temperature of  $T \approx 2$  K. The CO<sub>2</sub> concentration was about 1–1.5%, while ethanol was introduced into the gas phase by placing about 0.5 mL of pure liquid ethanol immediately behind the pulsed valve. For the rare isotopic species, isotopically pure <sup>13</sup>CO<sub>2</sub>, C<sup>18</sup>O<sub>2</sub>, <sup>13</sup>CH<sub>3</sub>CH<sub>2</sub>OH, CH<sub>3</sub><sup>13</sup>CH<sub>2</sub>OH, and CH<sub>3</sub>CH<sub>2</sub>OD were used in the same concentrations as the parent isotopic species.

At the start of the investigation, a CP-FTMW spectrum with a total of 650 000 free induction decays (FIDs) was recorded and averaged, in which 10 FIDs were acquired during each gas pulse. Following the taxonomy procedure,<sup>15</sup> signals arising from ethanol monomer and dimer and Ar/Ne clusters were assigned, and instrumental artifacts were discarded. The resulting spectrum is shown in Figure 1.

To identify the carriers of the unassigned signals in the CP spectrum, structures for the EDA and hydrogen-bonded complexes were optimized at the WB97XD/aug-cc-pVDZ level of theory and basis set using Gaussian 09 (see Figure 3).<sup>19</sup> Dipole moments and relative energies were calculated using the WB97XD/aug-cc-pVDZ structure at the CCSD(T)/aug-cc-pVQZ level of theory and basis set. These values and the predicted spectroscopic constants are summarized in Table 1. The calculated EDA structure agrees well with previous theoretical studies.<sup>14,20</sup> Using these structures, a preliminary prediction for the spectrum was generated with the CALPGM suite of programs<sup>21</sup> using a Watson-S Hamiltonian in the I' representation (Figure 2a).

Double-resonance (DR) cross-correlation<sup>15</sup> experiments were then performed on the ~50 most intense unidentified lines using the cavity FTMW instrument. Briefly, the intensity of each line was monitored in the cavity while a second (probe) radiation source, perpendicular to the expansion, was

**Table 1.** Theoretical Rotational Constants for the Hydrogen-Bonded (H-bond) and EDA Configurations<sup>a</sup> and Experimental Rotational Constants of CH<sub>3</sub>CH<sub>2</sub>OH–CO<sub>2</sub>

constant	calcd		exptl <sup>b</sup>	obs. – calc.	
	H-bond	EDA	CH <sub>3</sub> CH <sub>2</sub> OH–CO <sub>2</sub>	H-bond	EDA
A (MHz)	5220	6089	6128.018(1)	908	39
B (MHz)	1591	1722	1677.2492(2)	86	–45
C (MHz)	1406	1365	1340.84697(8)	–65	–24
μ <sub>a</sub>	–1.34	–0.93			
μ <sub>b</sub>	1.18	1.87			
μ <sub>c</sub>	0.59				
E <sub>rel</sub> (kJ/mol)	7.1	0.0			

<sup>a</sup>Calculated at the WB97XD/aug-cc-pVDZ level of theory and basis set. <sup>b</sup>The full set of experimental constants are given in Table S1 of the Supporting Information.

sequentially tuned to the frequency of every other unidentified line. If the two transitions (monitor and probe) shared an energy level, a substantial change in the intensity of the cavity (monitor) transition was observed. Linked transitions can only arise from the same molecular species and provide useful starting information to fit the rotational constants. Most prominent among the linkages measured in this experiment were a set of strong lines at 8.99, 11.89, and 14.74 GHz (Figure 2b). The simulated spectrum from the theoretical structure predicts strong  $K_a = 0$ , a-type transitions at 9.18, 12.14, 15.04 GHz, within 2% of the measured frequencies. A fit was performed using these frequencies, assuming that they arose from these transitions of the CH<sub>3</sub>CH<sub>2</sub>OH–CO<sub>2</sub> complex, and fitting only the B and C rotational constants (Figure 2c).

Once a preliminary assignment was made for the main species using the CP-FTMW spectra, many additional lines were readily identified. These lines, along with the previously assigned a-type transitions, were remeasured using the high-resolution cavity instrument. Additional, still weaker lines were then measured to refine the spectroscopic parameters (Figure 2d) using a separate cavity FTMW instrument operating from 5 to 40 GHz. No evidence of rotational transitions arising from internal rotation of the R–CH<sub>3</sub> group was observed.

## RESULTS AND DISCUSSION

In addition to the main isotopologue, the rotational spectra of <sup>13</sup>CH<sub>3</sub>CH<sub>2</sub>OH–CO<sub>2</sub>, CH<sub>3</sub><sup>13</sup>CH<sub>2</sub>OH–CO<sub>2</sub>, CH<sub>3</sub>CH<sub>2</sub>OD–CO<sub>2</sub>, CH<sub>3</sub>CH<sub>2</sub>OH–<sup>13</sup>CO<sub>2</sub>, and CH<sub>3</sub>CH<sub>2</sub>OH–C<sup>18</sup>O<sub>2</sub> were measured. Predictions for the rare isotopic species were

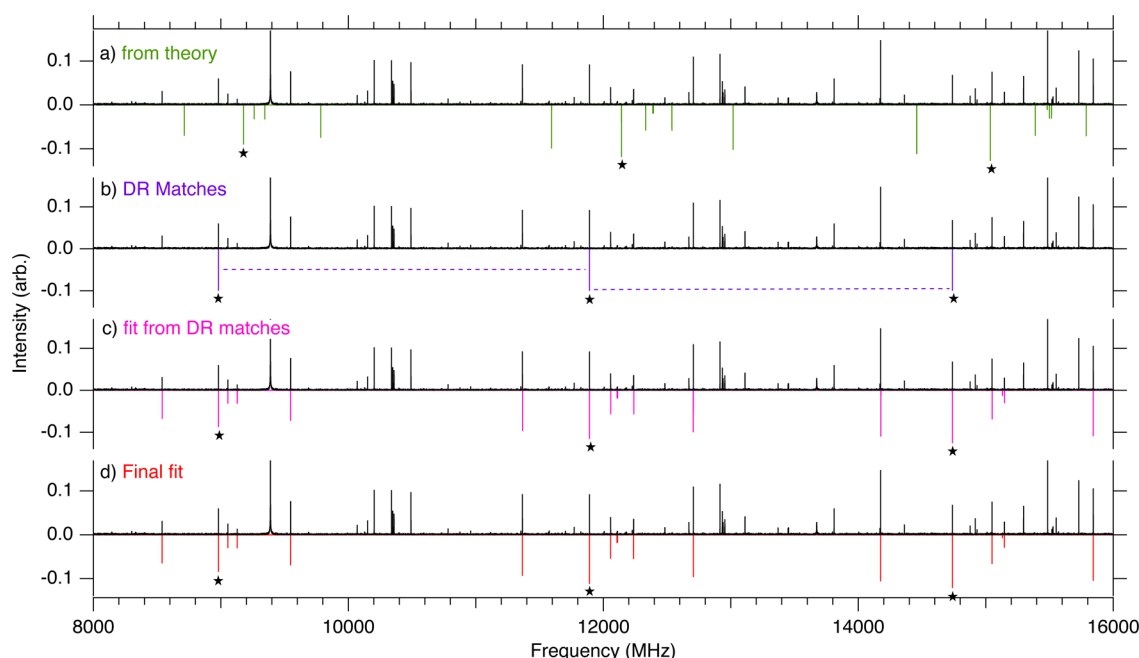
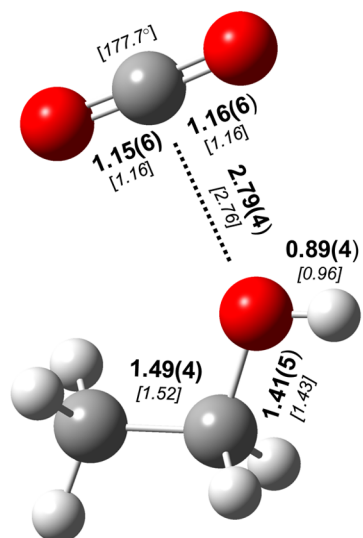


**Figure 2.** Visual representation of assignment and fitting process using DR linkages. (a) Observed spectrum in black along with the predicted spectrum of the  $\text{CH}_3\text{CH}_2\text{OH}-\text{CO}_2$  dimer from theoretical structure in green; (b) transitions definitively linked by DR during the taxonomy procedure in purple; (c) predicted spectrum in magenta after fitting the three linked transitions; (d) final fit to the experimental spectrum in red, refined using cavity FTMW measurements of 33 lines in the range of the instrument. Black stars highlight the three  $K_a = 0$ , a-type transitions that were identified by DR and used to anchor the assignment process. All simulations were performed at 2 K.

### Electron Donor-Acceptor



### Hydrogen Bonded

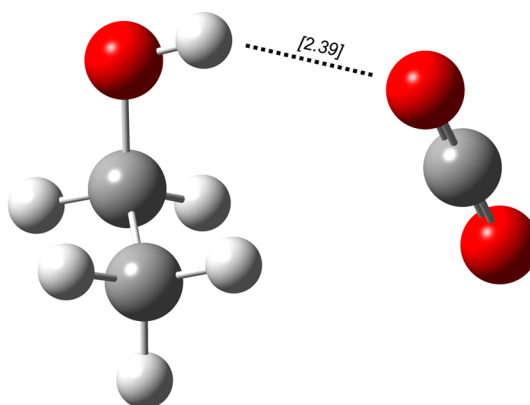


**Figure 3.** (Left) Semiexperimental structure ( $r_e^{\text{se}}$ ) for the EDA complex obtained in this work by a combination of isotopic substitution and theoretical vibrational corrections. (Right) Equilibrium geometry optimized in this work at the WB97XD/aug-cc-pVDZ level of theory for the hydrogen-bonded complex; the calculated hydrogen bond length is highlighted for comparison to the EDA bond. Uncertainties are given in parentheses in units of the last significant digit. For both structures, bond lengths are given in Å, bolded values are those of the  $r_e^{\text{se}}$  structure, and calculated values are given in brackets.

significantly more accurate after scaling the calculated rotational constants for each species by the ratio of the experimental to calculated constants for the parent isotopic species.<sup>22</sup> As a result, the isotopic lines could be rapidly measured in the cavity instrument without the need for the analogous CP-FTMW spectrum. With the exception of  $\text{CH}_3\text{CH}_2\text{OD}-\text{CO}_2$ , 20–40 transitions were measured and fit for each isotopologue, and

the root-mean-square of the fit converged to  $\leq 1.3$  kHz in all cases.

The best-fit parameters and the fit statistics are summarized in Table S1 of the [Supporting Information](#), while the measured rotational transitions of each isotopologue are given in the [Supporting Information](#) files in CALPGM (SPFIT/SPCAT) format.

On the basis of a comparison to the calculated and experimental rotational constants in Table 1, it is abundantly clear that the experimental structure is that of the EDA complex and not the hydrogen-bonding complex. The measurement of the spectra from the isotopically substituted species confirms the assignment to the EDA complex structure. As well, the measurement of isotopic species allows for a partial, semi-experimental structure ( $r_e^{se}$ ) to be determined using the STRFIT software.<sup>23</sup> In this procedure, the experimental rotational constants ( $A_0$ ,  $B_0$ ,  $C_0$ ) were corrected for zero-point vibrational effects as calculated at the MP2/aug-cc-pVDZ level of theory and basis set, producing semiexperimental constants ( $A_e^{se}$ ,  $B_e^{se}$ ,  $C_e^{se}$ ) that were then used in the structure determination. The five isotopically substituted species gave a total of 15 independent parameters ( $A$ ,  $B$ ,  $C$  for each), as well as those for the main species. Using these parameters, the bond lengths between all heavy atoms were fit, as well as those between the hydroxyl hydrogen and oxygen and between the ethanol and the  $\text{CO}_2$  subunits. No angles were constrained. The resulting structure, best-fit structural parameters, and uncertainties are summarized in Figure 3; the structure is given in Cartesian coordinates in Table S2 of the Supporting Information. Any parameters not fit directly were held fixed to their calculated values.

The torquing of the  $\text{O}=\text{C}=\text{O}$  bond from linear geometry and the resulting induced dipole moment is thought to be a primary factor in the increased ability of  $\text{scCO}_2$  to solvate polar molecules. The lack of commercial samples of  $^{18}\text{OC}^{16}\text{O}$ , however, precluded a direct determination of the  $\text{O}=\text{C}=\text{O}$  bond angle, and this angle was instead fixed to the value determined in the theoretical calculations carried out for this work:  $177.7^\circ$ . In an effort to indirectly test whether  $\text{CO}_2$  adopts a slightly nonlinear geometry, we attempted to fit the structure using a fixed  $\text{O}=\text{C}=\text{O}$  angle of  $180^\circ$ . The fit did not converge, and we take this as indirect experimental evidence of the slight nonlinearity of the  $\text{O}=\text{C}=\text{O}$  unit.

It is worth noting that the spectroscopic constants for  $\text{CH}_3\text{CH}_2\text{OD}-\text{CO}_2$  are significantly less accurate compared to those derived for other isotopologues, in part due to the small number of resolvable hyperfine transitions within our frequency coverage. The uncertainties in the  $r_e^{se}$  structure, however, are greatly reduced by including this species in the structural analysis. Still, its associated uncertainties limit the absolute accuracy with which the structural parameters can be derived. The sensitivity of the structure to the inclusion of the  $\text{CH}_3\text{CH}_2\text{OD}-\text{CO}_2$  species may imply that the  $\text{O}-\text{H}$  bond length and  $\text{C}-\text{O}-\text{H}$  angle are poorly constrained compared to the heavy-atom backbone. Extending the frequency range and number of measured rotational transitions for  $\text{CH}_3\text{CH}_2\text{OD}-\text{CO}_2$  would likely better constrain the fit and improve the accuracy of the resulting  $r_e^{se}$  structure. Regardless, the derived structure is more than adequate to unambiguously establish an EDA configuration.

Finally, no evidence was found in our broadband spectrum for the hydrogen-bonded complex, and furthermore, no signal was detected from this conformer during a targeted search with the cavity instrument. Less than 10 lines of any appreciable intensity remain unassigned in the CP-FTMW spectrum, and these may arise from  $\text{Ar/Ne}$  clusters with  $\text{CO}_2$  or  $\text{CH}_3\text{CH}_2\text{OH}$ . As such, these finding may indicate a low barrier to isomerization between the two conformers; however, further theoretical analysis of the potential energy surface would be required to critically explore this possibility.

## CONCLUSIONS

In conclusion, previous experimental and theoretical studies have suggested that the primary interaction between ethanol and  $\text{CO}_2$  when ethanol is used as a cosolvent in  $\text{scCO}_2$  is through the formation of an EDA complex. To critically assess this explanation, we have recorded the spectrum of the gas-phase  $\text{CH}_3\text{CH}_2\text{OH}-\text{CO}_2$  dimer, to our knowledge the first study of the isolated complex. High-level quantum-chemical calculations suggest the EDA complex to be energetically more stable compared to the hydrogen-bonded complex. By observing and characterizing the rotational spectra of normal and isotopically substituted isotopologues of the complex, we have unambiguously established that the observed spectra arise from  $\text{CH}_3\text{CH}_2\text{OH}-\text{CO}_2$  in an EDA configuration; no evidence is found for the hydrogen-bonded complex, despite dedicated laboratory searches.

## ASSOCIATED CONTENT

### Supporting Information

The Supporting Information is available free of charge on the ACS Publications website at DOI: 10.1021/acs.jpca.7b06103.

File of measured transitions for  $\text{CH}_3\text{CH}_2\text{OD}-\text{CO}_2$  (TXT)

File of measured transitions for  $\text{CH}_3\text{CH}_2\text{OH}-^{13}\text{CO}_2$  (TXT)

File of measured transitions for  $\text{CH}_3\text{CH}_2\text{OH}-^{18}\text{OC}^{18}\text{O}$  (TXT)

File of measured transitions for  $\text{CH}_3\text{CH}_2\text{OH}-\text{CO}_2$  (TXT)

File of measured transitions for  $\text{CH}_3^{13}\text{CH}_2\text{OH}-\text{CO}_2$  (TXT)

Experimental rotational constants for all measured ethanol- $\text{CO}_2$  species and Cartesian coordinates of the structure of the  $\text{CH}_3\text{CH}_2\text{OH}-\text{CO}_2$  dimer (PDF)

File of measured transitions for  $^{13}\text{CH}_3\text{CH}_2\text{OH}-\text{CO}_2$  (TXT)

## AUTHOR INFORMATION

### Corresponding Authors

\*E-mail: bmcguire@nrao.edu (B.A.M.).

\*E-mail: mccarthy@cfa.harvard.edu (M.C.M.).

### ORCID

Brett A. McGuire: 0000-0003-1254-4817

Michael C. McCarthy: 0000-0001-9142-0008

### Present Address

<sup>§</sup>M.-A.M.-D.: Institut des Sciences Moléculaires d'Orsay, CNRS, Univ. Paris Sud, Université Paris-Saclay, Orsay, France.

### Notes

The authors declare no competing financial interest.

<sup>¶</sup>B.A.M. is a Jansky Fellow of the National Radio Astronomy Observatory.

## ACKNOWLEDGMENTS

B.A.M. thanks G. A. Blake for access to computing resources, K. L. K. Lee for helpful discussions regarding the theoretical treatments, and Z. Kisiel for insights into the STRFIT program. The National Radio Astronomy Observatory is a facility of the National Science Foundation operated under cooperative agreement by Associated Universities, Inc. This work was partially supported by award NSF-CHE-1566266.



## REFERENCES

- (1) Hannay, J. B.; Hogarth, J. On the solubility of solids in gases. *Proc. R. Soc. London* **1879**, 29, 324–326.
- (2) Zosel, K. Separation with supercritical gases - practical applications. *Angew. Chem., Int. Ed. Engl.* **1978**, 17, 702–709.
- (3) Hubert, P.; Vitzthum, O. G. Fluid extraction of hops, spices, and tobacco with supercritical gases. *Angew. Chem., Int. Ed. Engl.* **1978**, 17, 710–715.
- (4) Schaeffer, S. T.; Zalkow, L. H.; Teja, A. S. Extraction of monocrotaline from *crotalaria spectabilis* using supercritical carbon dioxide and carbon dioxide-ethanol mixtures. *Biotechnol. Bioeng.* **1989**, 34, 1357–1365.
- (5) Gearhart, J. A.; Garwin, L. ROSE Process Improves Resid Feed; 1976; Vol. 55, pp 125–129.
- (6) Dobbs, J. M.; Wong, J. M.; Lahiere, R. J.; Johnston, K. P. Modification of supercritical fluid phase behavior using polar cosolvents. *Ind. Eng. Chem. Res.* **1987**, 26, 56–65.
- (7) Rudyk, S.; Hussain, S.; Spirov, P. Supercritical extraction of crude oil by methanol- and ethanol-modified carbon dioxide. *J. Supercrit. Fluids* **2013**, 78, 63–69.
- (8) Ilyushin, V. V.; Lovas, F. J.; Plusquellic, D. F. Microwave spectrum of the heterodimers:  $\text{CH}_3\text{OH}-\text{CO}_2$  and  $\text{CH}_3\text{OH}-\text{H}_2\text{CO}$ . *J. Mol. Spectrosc.* **2006**, 239, 94–100.
- (9) Stubbs, J. M.; Siepmann, J. I. Binary phase behavior and aggregation of dilute methanol in supercritical carbon dioxide: A Monte Carlo simulation study. *J. Chem. Phys.* **2004**, 121, 1525–11.
- (10) Chatzis, G.; Samios, J. Binary mixtures of supercritical carbon dioxide with methanol. A molecular dynamics simulation study. *Chem. Phys. Lett.* **2003**, 374, 187–193.
- (11) Xu, W.; Yang, J.; Hu, Y. Microscopic structure and interaction analysis for supercritical carbon dioxide-ethanol mixtures: A Monte Carlo simulation study. *J. Phys. Chem. B* **2009**, 113, 4781–4789.
- (12) Mani, D.; Arunan, E. The  $\text{X}-\text{C}\cdots\text{Y}$  ( $\text{X} = \text{O}/\text{F}$ ,  $\text{Y} = \text{O}/\text{S}/\text{F}/\text{Cl}/\text{Br}/\text{N}/\text{P}$ ) ‘carbon bond’ and hydrophobic interactions. *Phys. Chem. Chem. Phys.* **2013**, 15, 14377–7.
- (13) Skarmoutsos, I.; Dellis, D.; Samios, J. Investigation of the local composition enhancement and related dynamics in supercritical  $\text{CO}_2$ -cosolvent mixtures via computer simulation: The case of ethanol in  $\text{CO}_2$ . *J. Chem. Phys.* **2007**, 126, 224503–11.
- (14) Saharay, M.; Balasubramanian, S. Electron donor-acceptor interactions in ethanol- $\text{CO}_2$  mixtures: An *ab initio* molecular dynamics study of supercritical carbon dioxide. *J. Phys. Chem. B* **2006**, 110, 3782–3790.
- (15) Crabtree, K. N.; Martin-Drumel, M.-A.; Brown, G. G.; Gaster, S. A.; Hall, T. M.; McCarthy, M. C. Microwave spectral taxonomy: A semi-automated combination of chirped-pulse and cavity Fourier-transform microwave spectroscopy. *J. Chem. Phys.* **2016**, 144, 124201–13.
- (16) Balle, T. J.; Flygare, W. H. Fabry–Perot cavity pulsed Fourier transform microwave spectrometer with a pulsed nozzle particle source. *Rev. Sci. Instrum.* **1981**, 52, 33–45.
- (17) Brown, G. G.; Dian, B. C.; Douglass, K. O.; Geyer, S. M.; Shipman, S. T.; Pate, B. H. A broadband Fourier transform microwave spectrometer based on chirped pulse excitation. *Rev. Sci. Instrum.* **2008**, 79, 053103–14.
- (18) Loru, D.; Peña, I.; Sanz, M. E. Ethanol dimer: Observation of three new conformers by broadband rotational spectroscopy. *J. Mol. Spectrosc.* **2017**, 335, 93–101.
- (19) Frisch, M. J.; Trucks, G. W.; Schlegel, H. B.; Scuseria, G. E.; Robb, M. A.; Cheeseman, J. R.; Scalmani, G.; Barone, V.; Mennucci, B.; Petersson, G. A.; et al. *Gaussian 09*, revision B.01; Gaussian, Inc.: Wallingford, CT, 2009.
- (20) Danten, Y.; Tassaing, T.; Besnard, M. Vibrational spectra of  $\text{CO}_2$  electron donor-acceptor complexes from *ab initio*. *J. Phys. Chem. A* **2002**, 106, 11831–11840.
- (21) Pickett, H. M. The fitting and prediction of vibration-rotation spectra with spin interactions. *J. Mol. Spectrosc.* **1991**, 148, 371–377.
- (22) Carroll, P. B.; McGuire, B. A.; Zaleski, D. P.; Neill, J. L.; Pate, B. H.; Widicus Weaver, S. L. The pure rotational spectrum of glycolaldehyde isotopologues observed in natural abundance. *J. Mol. Spectrosc.* **2013**, 284–285, 21–28.
- (23) Kisiel, Z. Least-squares mass-dependence molecular structures for selected weakly bound intermolecular clusters. *J. Mol. Spectrosc.* **2003**, 218, 58–67.